Post-irradiation examinations of annular mixed oxide (MOX) fuel pins for sodium fast reactors

Fabiola Cappia – Idaho National Laboratory – fabiola.cappia@inl.gov
Jason Harp – Idaho National Laboratory – jason.harp@inl.gov

A more systematic study of the performance of annular fuel MOX pins has been undertaken in this project, with the specific objective both to ameliorate the understanding of the effects of irradiation temperature and burnup on the fuel microstructural evolution and to provide supporting data for validation of fuel-performance models.

The primary goal of Generation IV nuclear energy systems is to improve resource utilization and to minimize the nuclear waste burden while improving safety, reliability and proliferation resistance. In addition, through innovation aimed at reducing capital costs and financial risks, Gen IV technologies will provide clean energy at competitive costs compared to other energy sources [1].

The sodium-cooled fast reactor (SFR) is one of the six technologies that has been chosen as a next-generation nuclear energy system to meet these goals. SFR technology has been historically established both through pioneering experimental reactors (e.g., Fermi, Experimental Breeder Reactor-II, Rapsodie) and prototype reactors (e.g., Phenix, BN-600, Monju). Past experience is an essential asset and provides the basis to further develop advanced SFR concepts [2].

In terms of fuel for SFR, initial efforts in the fifties were focused on metallic fuels, due to the highest heavy-metal density favoring the highest breeding ratio. However, metal fuels struggled in achieving high burnup due to excessive swelling and dimensional instability. In a short time, uranium and plutonium mixed oxide (MOX) fuels became the reference fuel for SFR, thanks to their good stability under irradiation. Since the sixties, hundreds of thousands of pins have been successfully irradiated up to burnups exceeding 20% fission of initial heavy-metal atom [3]. High linear heat-generation rates (>30 kW/m) and high burnup, typically above 15%, were the main objectives of SFR fuel research and development, because it was shown that increasing fuel burnup offers significant cost advantages. Annular pellets, which lower the smear density to compensate for increasing pellet swelling as burnup progresses and maximize power rating for a prescribed margin to fuel melting [4], are one of the promising designs for SFR driver fuel.

Irradiation experiments of advanced MOX test assemblies were conducted in the Fast Flux Test Facility (FFTF) between 1980 and 1993 [5]. Assembly FO-2, which was one of the first assemblies to use HT-9 as cladding material, was designed to

Design parameters		K-type	L-type
Cladding	Material	HT-9	HT-9
	Outer diameter (mm)	6.858	6.858
	Cladding thickness (mm)	0.533	0.533
	Plenum volume (cm^3)	23.6	23.6
Fuel Pellet	Material	MOX	MOX
	Outer diameter (mm)	5.59	5.59
	Inner diameter (mm)	1.397	1.397
	Pellet length range (mm)	6.27 to 8.66	6.27 to 8.66
	Gap width (mm)	0.203	0.203
	Smeared density (%TD)	80±1	80±1
	Pellet density (%TD)	91.7	91.7
	Oxygen-to-metal ratio	1.96±0.010	1.96±0.010
	Pu content (Pu/(Pu+U) wt%)	22	26

Table 1. Design parameters of the FFTF pins.

evaluate the effects of fuel form (i.e. annular vs solid) and fuel-design variables on pin performance. The test assembly was irradiated for 312 equivalent full power days at peak power of 45.6 kW/m, peak burnup of 65.2 GWd/tHM and peak fast fluence of 9.9×10^{22} n/cm2. Initial post-irradiation examination (PIE) of the overall assembly and selected pins showed good and predictable performance of MOX with HT-9 cladding [6]. However, data remain limited to two studies of single pins [6,7]. A more systematic study of the performance of MOX annular fuel pins has been undertaken in this project, with the specific objective both to ameliorate the understanding of the effects of irradiation temperature and burnup on the fuel microstructural evolution and to provide supporting data for validation of fuel-performance models.

Project Description

In the FO-2 assembly, there were 12 different fuel variants. Ten variants were solid MOX pellets and 2 were annular MOX pellets. This work focuses only on the annular variants. Four pins of two different types were selected: two of the L-type and two of the K-type. Design parameters of each pin are summarized in Table 1. The two types of pins have the same nominal design data, except for the initial Pu content, which is 26 wt% for the L-type and 22 wt% for the K-type.

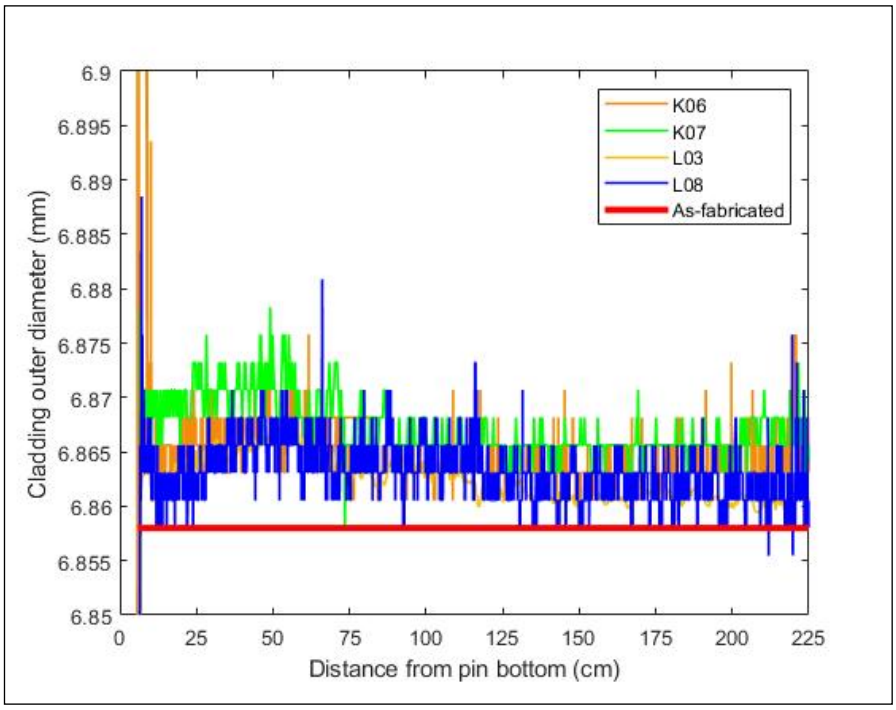

Figure 1. Cladding profilometry results of the four pins.

PIEs are primarily performed at the Hot Fuel Examination Facility (HFEF) of Idaho National Laboratory (INL). All non-destructive PIEs were completed, and destructive baseline PIEs are currently ongoing. Baseline non-destructive PIEs performed included neutron radiography, gamma spectroscopy, and dimensional inspection. Baseline destructive PIEs comprise fission-gas release, burnup analysis, and optical microscopy, including image analysis and micro-hardness testing.

PIE highlight and discussion

Non-destructive PIE

Spiral profilometry scans were collected utilizing the in-cell element contact profilometer (ECP). The diameter was measured at intervals of 2.54 mm, starting at the top of each fuel pin. Results are reported for all four pins in Figure 1. The nominal as-fabricated diameter is also shown in red. The results of all four pins are similar, with a uniform and limited strain along the full pin length. A more pronounced swelling of the cladding is noticeable in the part corresponding to the active column length, which is expected.

Gamma spectroscopy was performed with the precision gamma scanner (PGS) at HFEF. Only long-lived fission products Eu-154 and Cs-137 were detectable. Eu-154 and Cs-137 axial profiles are presented in Figure 2 and 3, respectively. The Eu-154 profiles follow the fission density of the fuel, indicating that the pins achieved similar burnup values, with pin L-08 having slightly higher burnup value. The depressed signals above and below the active fuel stack (see red arrows in Figs. 2 and 3) correspond to the blanket portions of the stack. According to fuel-performance-code calculations, burnup values at peak

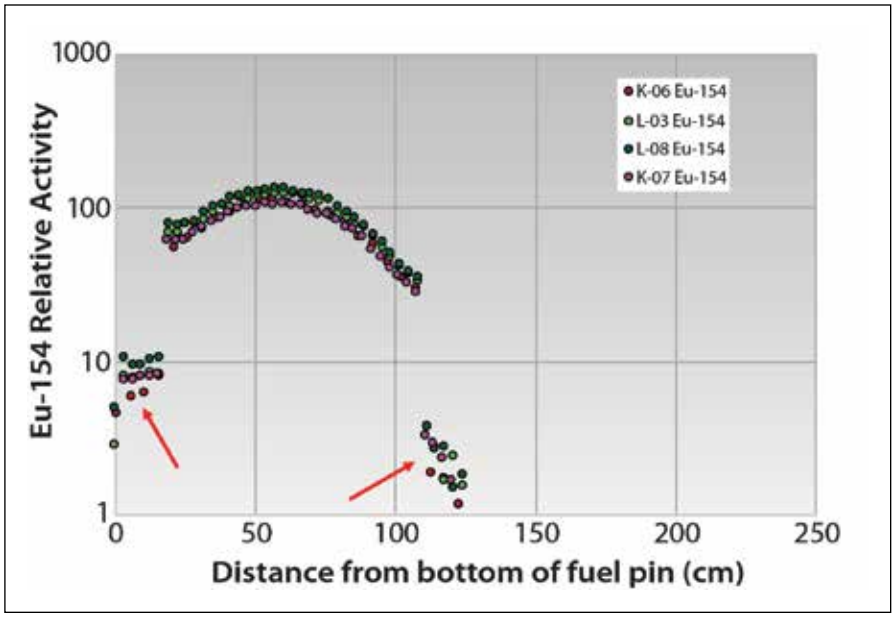

Figure 2. Axial gamma scanning (Eu-154) of the four pins.

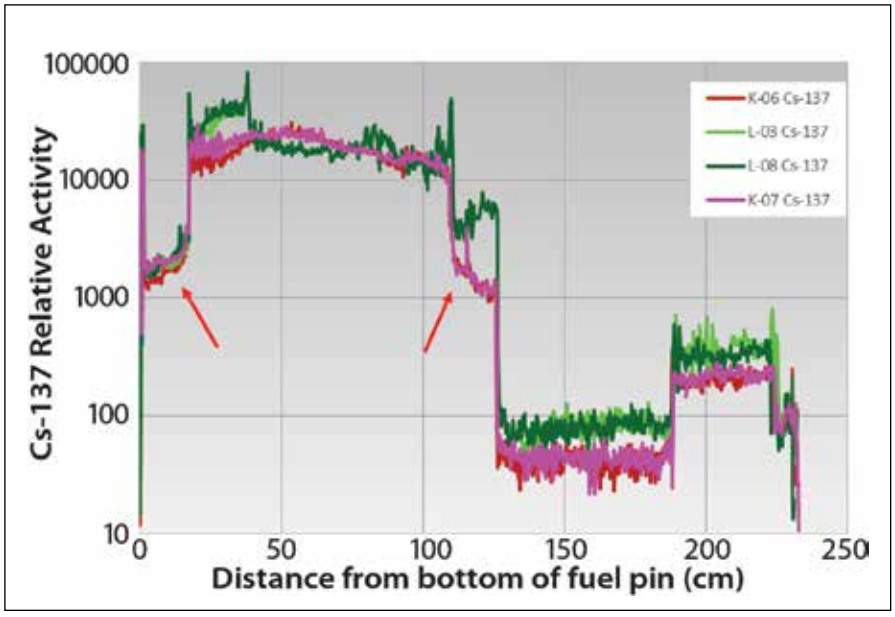

Figure 3. Axial gamma scanning (Cs-137) of the four pins.

power node are 59.4 GWd/tHM for K06 and K07, 59.5 GWd/tHM for L03 and 62 GWd/tHM for L08. Burnup analyses are ongoing in order to compare and verify the calculations. The Cs profiles of the K-type pins are consistent and resemble the as-generated profile. A remarkable difference is visible in the behavior of Cs in the L-type pins, compared to the other two pins. Depletion of Cs has occurred in the central part of the active column, and Cs redistribution has occurred towards the end of the fuel, particularly towards the first 1/3 of the fuel length.

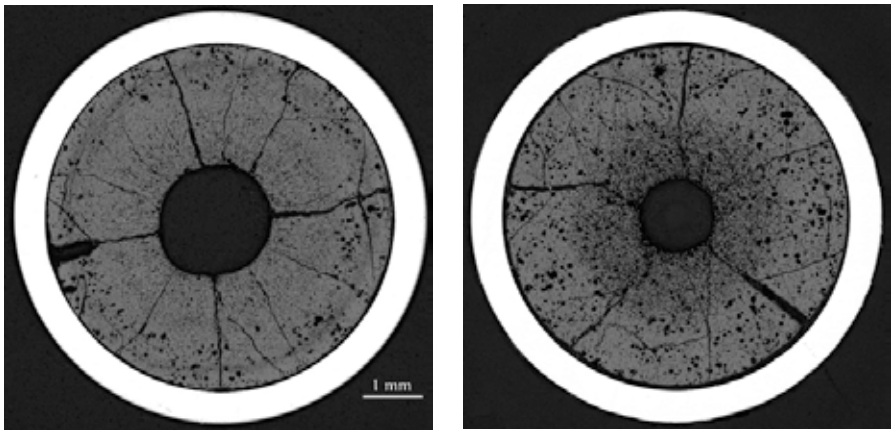

Figure 4. Low magnification cross section images (50x) from pin K06 at different axial positions. (a) Relative axial position 0.5 (peak power node) and (b) 0.05.

Destructive PIE

Major changes were implemented in the procedure to prepare metallography samples for these pins as compared to previous PIE investigations carried out on FO-2 pins. It is known that with increasing burnup, part of the fission products, particularly cesium and molybdenum, leave the fuel matrix and accumulate in the fuel-to-cladding gap, forming the so-called joint oxyde gaine (JOG) [3]. Historical electron probe microanalyzer (EPMA) data [8] and thermodynamic calculations [9] suggest Cs_2MoO_4 as one of the major components of the JOG. The compound is highly hygroscopic and tends to dissolve rapidly when in contact with water, which was the main cutting fluid used in the past. The new sample preparation procedure uses non-water-based solutions and cleaning with ethanol—thus allowing

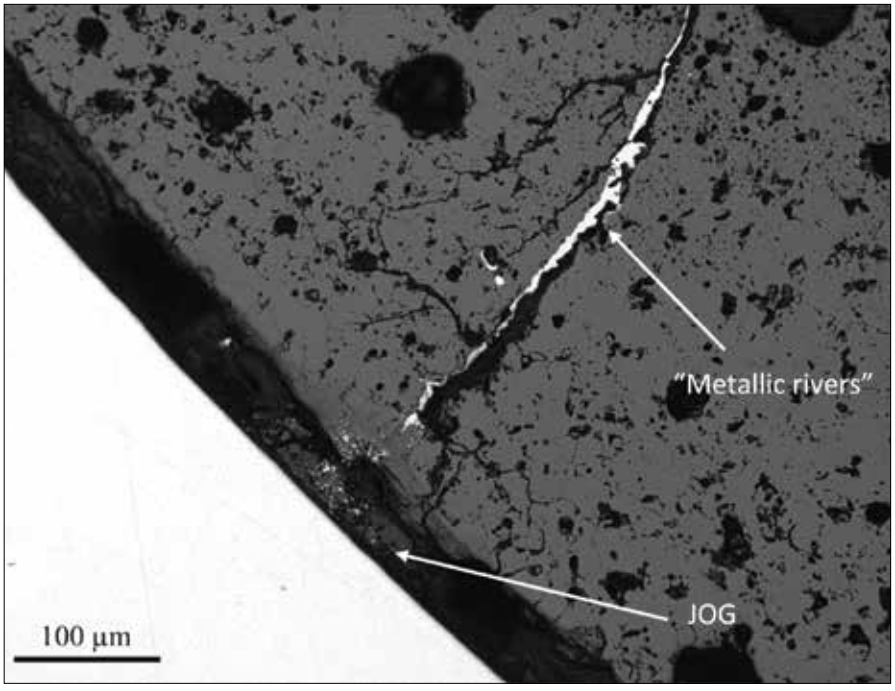

Figure 5. High-magnification image (200×) showing the formation of JOG and metallic rivers around one of the fuel cracks.

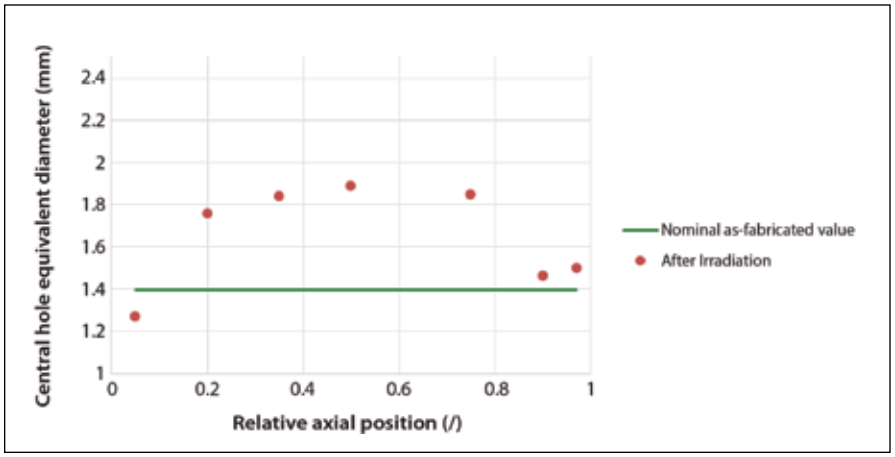

Figure 6. Evolution of the central void size after irradiation in pin K06. Increase of the void size is a consequence of pore migration induced by thermal gradients. Decrease of the size is due to possible material relocation or migration towards the coldest part of the pin.

better sample preparation compared to the past [10] and preserving both the JOG and the fission products accumulating in the fuel-cladding chemical interaction (FCCI) layer (Figure 5).

From optical microscopy images, engineering-scale measurements of the fuel microstructure features can be obtained. For instance, central void dimension and its evolution along the pin axis are reported in Figure 6. This type of quantitative information is fundamental to validate models of pore migration used in fuel performance codes [11].

Accomplishments

PIE results highlighted very good and comparable performance among the pins under similar irradiation conditions. Cesium redistribution has occurred in two of the pins, as shown in Figure 3. Cesium migration is a known phenomenon in SFR MOX fuels, induced by radial and axial temperature gradients. Cesium becomes volatile in the hottest parts of the fuel and migrates by successive evaporation and condensation to the colder regions, where lower temperatures allow formation of Cs compounds with low Cs vapor pressure [12]. Despite increased cesium concentration at specific axial locations, no enhanced cladding strain was measured, as shown in Figure 1, suggesting no detrimental impact on the cladding following cesium accumulation, at least at intermediate burnup.

Fuel microstructure evolution occurs both radially and axially, depending on the local temperatures and burnup levels. At peak-power axial-node positions (i.e., at intermediate relative axial positions), formation of columnar grains occurs where temperatures exceed 1800–1900°C [4], as shown in Figure 4a. An enlargement of the as-fabricated annulus occurs due to pore migration, driven by steep temperature gradients (Figure 6). At the beginning of the fuel column, where power and burnup levels remain lower, no columnar grain formation occurs (Figure 4b), but the central part of the pellet shows a different texture, probably related to the enhanced diffusion-driven precipitation of fission products on grain boundaries.

Analysis of the optical microscopy mounts at different axial locations showed that the gap is still open. Partially, the gap is filled with fission

Regarding the destructive tests, a major accomplishment has been obtained by implementing a new sample-preparation methodology, which considerably improved the quality of the samples.

products that migrated radially. Present data confirmed that formation of the JOG occurs already at intermediate burnup, as indicated in Figure 5. The FCCI includes metallic precipitates (white particles in Figure 5) that could be either metallic fission products or cladding components. In addition, metallic rivers [13] are observed along fuel cracks. Advanced PIE such as scanning electron microscopy and energy-dispersive X-ray spectroscopy are foreseen to determine the chemical composition of the observed phases.

PIE results on four pins with advanced annular MOX and HT-9 cladding have been gathered. The non-destructive examination did not reveal anomalous behavior of the pins and are in line with previous investigations on similar pins.

Regarding the destructive tests, a major accomplishment has been obtained by implementing a new sample-preparation methodology, which considerably improved the quality of the samples. In particular, the JOG and FCCI have been preserved for the first time in FFTF annular MOX fuels. While the JOG and the FCCI have been extensively characterized at very high burnup [8], less it is known about the composition and structure of these phases at intermediate burnup. The present data will allow the characterization of the FCCI at intermediate burnup and comparison with published literature.

Publications

[1.] OECD Nuclear Energy Agency, Technology Roadmap Update for Generation IV Nuclear Energy Systems, 2014.

[2.] K. Aoto, P. Dufour, Y. Hongyi, J.P. Glatz, Y. Kim, Y. Ashurko, R. Hill, N. Uto, Prog. Nucl. Energy 77 (2014) 247–265.

[3.] Y. Guerin, in:, Compr. Nucl. Mater., Elsevier, 2012, pp. 547–578.

[4.] N.E. Todreas, M.S. Kazimi, in:, Taylor & Francis, 1990, p. 317.

[5.] J. Perez-Carter, N.J. Graves, B.C. Gneiting, Irradiation History Report for Advanced Oxide Fuel Assembly FO-2, 1993.

[6.] L.L. Gilpin, R.B. Baker, S.A. Chastain, in:, ANS Annu. Meet. 1989, Atlanta, 1989.

[7.] M. Teague, B. Gorman, J. King, D. Porter, S. Hayes, J. Nucl. Mater. (2013).

[8.] M. Tourasse, M. Boidron, B. Pasquet, J. Nucl. Mater. (1992).

[9.] J.-C. Dumas, Etude Des Conditions de Formation Du Joint-Oxyde-Gaine Dans Les Combustibles Oxydes Mixtes Des Reacteurs a Neutrons Rapides, Observations et Proposition D'un Modele de Comportement Des Produits de Fission Volatils, Institut National Polytechnique de Grenoble, 1995.

[10.] M. Teague, Post Irradiation Examination of Legacy FFTF Oxide Fuel, 2012.

[11.] S. Novascone, P. Medvedev, J.W. Peterson, Y. Zhang, J. Hales, J. Nucl. Mater. 508 (2018) 226–236.

[12.] W. Breitung, G. Schumacher, The Significance of Cesium in LMFBR and LWR Safety Analysis, 1984.

[13.] R.B. Fitts, E.L. Long, J.M. Leitnaker, in:, Fast React. Fuel Elem. Technol., 1971, pp. 431–458.

Distributed Partnership at a Glance	
NSUF and Partners	Facilities and Capabilities
Idaho National Laboratory	Hot Fuel Examination Facility (HFEF)
Collaborators	
Idaho National Laboratory	Fabiola Cappia (principal investigator), Jason Harp (principal investigator)